AUTOMATED CRATER DELINEATION. J. S. Marques[2] and P. Pina[2], [1]ISR, Instituto Superior Técnico, Lisbon, PORTUGAL (jsm@isr.ist.utl.pt), [2]CERENA, Instituto Superior Técnico, Lisbon, PORTUGAL (ppina@tecnico.ulisboa.pt).

Introduction: Crater detection algorithms (CDA) have greatly evolved in the last decade and are detecting much smaller structures with higher performances [1-3] which is permitting their use in the construction and upgrade of crater catalogues, namely for Mars [4] and Phobos [5]. Although improvements are still required in the CDA, namely for detecting metric craters in diameter with the same high performances, the algorithms already available are robust enough for large scale detections. Thus, the focus of attention can now be moved towards crater characterization, namely to establish a degree of preservation or erosion for each individual crater. The first step we are considering for establishing this issue consists in the delineation of the real contour of the crater, since CDA outputs describe each crater by perfect circular shapes, no matter its degree of erosion. Therefore, our current objective is to propose a robust algorithm able to deal with the automated delineation of impact craters of any size and degree of preservation, on a wide variety of terrains, and adequate for large scale delineations.

Previous algorithms: The delineation of the crater rim has been manually performed [6] and there are almost no algorithms in the literature addressing this problem. The exceptions are two exploratory approaches of ours: one based on a judicious sequence to find and link the crater edges in polar coordinates ('Polar') [7], the other based on the watershed transform and other mathematical morphology operators ('Morphologic') [8]. The results obtained on a small dataset from Mars achieved good rates [9] but when the dataset was enlarged, encompassing a wider diversity of terrain ages and textures, the performances were not preserved. The evident degradation of the performance in the most difficult examples showed us that there was still room for improvement.

Algorithm based on Edge Maps and Dynamic Programming: The algorithm devised processes the images in polar coordinates and is constituted by two main steps:

1. Edge enhancement, constructing an Edge Map based upon the intensity transitions along radial lines intersecting the center of the crater, and
2. Crater delineation, determining an optimal path from the minimization of an energy functional by Dynamic Programming.

The formalism of the algorithm is described in detail in [10].

Datasets: In the construction of the testing datasets we covered a large diversity of the Martian landscape and crater densities. We selected regions in both hemispheres, with noticeable differences in the amount of craters, also exhibiting a wide variety of preservation, from pristine craters (with sharp rims) to degraded structures (with irregular, faint or missing parts of the rim), and also examples of craters hardly noticeable. The datasets contain a total of 1045 craters acquired at two resolutions: 845 craters from HiRISE images and 240 craters from a THEMIS global mosaic, permitting analysing a wide and complementary range of crater dimensions. The HiRISE images (datasets 1 to 8) comprise craters selected from distinct Martian regions, with a maximum diameter of 1.1 km and going down to 5 and 10 meters for the smallest structures (20 pixels for the resolutions of 0.25 and 0.50 m/pixel, respectively). For the THEMIS Day IR 100m Global Mosaic images (dataset 9), the craters were extracted all around the planet, with diameters below 200 km until a minimum of 4 km (or 40 pixels). Although many craters smaller than those dimensions are undoubtedly perceived, we fixed an inferior limit to avoid ambiguous situations.

Delineation performances: We evaluated the performance of the algorithm through the comparison of the delineated contour with a ground-truth or manually created contour. Thus, each crater was individually analyzed and a closed contour estimated by the current algorithm ('Dynamic Programming') and also by one of the previous approaches ('Morphologic'). The 'Polar' algorithm was also tested but due to high amount of craters for which it did not propose a contour (in more than half of the dataset) we left it outside the comparisons. Exampes of the delineation outputs of the algorithm are presented in Figure 1. They are a comprehensive illustration of the performances achieved by the algorithm, since the level of accuracy attained is very precise. This is not only evident on craters where the rim is complete and clearly discernible, but also in situations where the rim is obliterated by other craters or only partially visible. This thorough correctness is generally observed in the whole dataset, independently of the dimension of the craters or of the sensor. On the contrary, the difficulties faced by the algorithm in estimating the contours are very less frequent and only partially incorrect in some sections of the rim. These situations concern mainly elliptical craters with very high eccentricity.

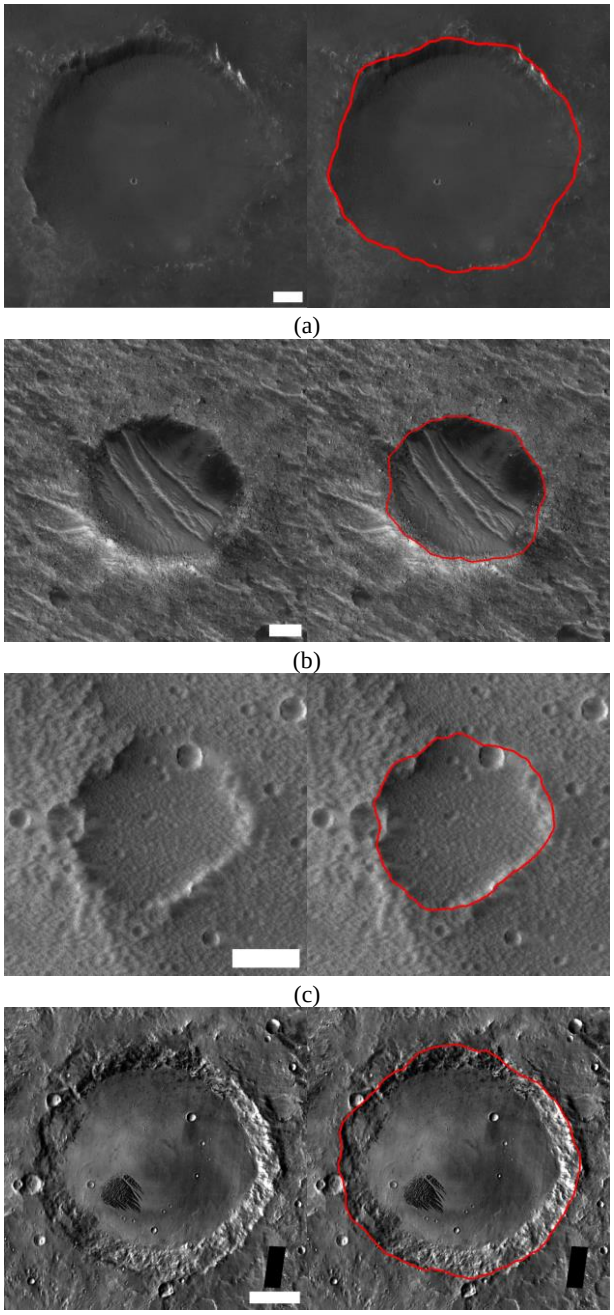

Figure 1. Crater delineation examples on (a-c) HiRISE and (d) THEMIS samples. Scale bars correspond to 50m in HiRISE and 20km in THEMIS [image credits: NASA/JPL/University of Arizona (HiRISE) and NASA/JPL-Caltech/Arizona State University]

The average performances obtained for each dataset with those two algorithms are presented in Table I. The overall error of 4.2% of incorrect delineations can be considered very good, also outperforming the performance of the other method (overall error of 10.9%). In particular, the average performance is a bit better for THEMIS images than for all HiRISE images (errors of 1.5% and 5.0%, respectively). Also, the average values for each individual HiRISE dataset show some normal fluctuation, due to the intrinsic characteristics of the different terrains, with errors between 2.5% and 11.9%. In comparison, the 'Morphologic' algorithm achieved always poorer individual performances performances in the 9 datasets.

Table 1. Crater delineation performances by dataset and global (error values in %).

#	Nb. craters	'Dyn. Prog.'	'Morpho'
1	60	2.5	9.6
2	100	8.4	13.6
3	110	2.7	9.4
4	65	11.9	19.9
5	100	3.8	8.6
6	120	5.2	8.9
7	135	3.3	9.6
8	115	4.8	8.6
9	240	1.5	11.1
1-8	805	5.0	10.5
1-9	240	4.2	10.7

Conclusions: The exploitation of the a priori knowledge about the problem, like the circular geometry and image intensity patterns of the craters, and its integration into an optimization procedure, are the key features for the robustness of the algorithm. In particular, the geometry of the craters permits to adequately define a region of interest around its rim and constrain the space of search for edges of interest. Moreover, the enhancement of the crater edges by the Edge Map and the detection of the optimal path (the crater contour) with the Dynamic Programming algorithm are also strong points. Finally, converting and processing the crater images into polar coordinates greatly simplifies the algorithm. In addition, the sensitivity tests we have performed, changing some parameters of the algorithm and positioning the circular masks in different locations, reinforce the high robustness of the algorithm.

References: [1] Bandeira et al. (2007) *IEEE TGRS, 45*, 4008-4015. [2] Martins et al. (2009) *IEEE GRSL, 6*, 127-131. [3] Bandeira et al (2012) *Adv. Spac. Res., 49*, 64-74. [4] Salamuniccar et al. (2011*) PSS, 59*, 111-131. [5] Salamuniccar et al. (2014) *Adv. Spac. Res., 53*, 1798-1809. [6] Mouginis-Mark P. J. et al. (2004) *JGR, 109*, E08006. [7] Marques J. S. and Pina P. (2013) *LNCS, 7887*, 213-220. [8] Pina P. and Marques J. S. (2013) *LNCS, 7950*, 717-725. [9] Pina P. and Marques J. S. (2013) *PCC4*, Abstract #1309. [10] Marques J. S. and Pina P. (2015) submitted.